# EVALUATION OF REMOTE SENSING-BASED IRRIGATED AREA MAP FOR THE CONTERMINOUS UNITED STATES

**Shahriar Pervez,** Scientist
Stinger Ghaffarian Technologies (SGT)
Contractor to the U.S. Geological Survey (USGS) Earth Resources Observation and Science (EROS) Center,
47914 252nd Street
Sioux Falls, South Dakota 57198
work performed under USGS contract 08HQCN0005
spervez@usgs.gov

**Jesslyn F. Brown,** Geographer
USGS EROS
47914 252nd Street
Sioux Falls, South Dakota 57198
jfbrown@usgs.gov

**Susan Maxwell,** Scientist
SGT, contractor to the USGS EROS
47914 252nd Street
Sioux Falls, South Dakota 57198
work performed under USGS contract 08HQCN0005
maxwell@usgs.gov

## ABSTRACT

We mapped irrigated areas of the conterminous United States using three sources of information: (1) county irrigation statistics from the U.S. Department of Agriculture (USDA) National Agricultural Statistics Service (NASS), (2) land cover information from the 2001 National Land Cover Database (NLCD), and (3) satellite imagery from the Moderate Resolution Imaging Spectroradiometer (MODIS) instrument. We have used a reproducible method where MODIS pixels with high annual peak Normalized Difference Vegetation Index (NDVI) values within agriculture land cover correspond to the reported irrigated area at the county level. We call this geospatial irrigation map the MODIS Irrigated Agriculture Dataset for the United States (MIrAD-US). This is the first irrigated area map of the conterminous United States at 250x250-$m^2$ spatial resolution, thus evaluation of the map is a challenge because no other maps are available at a national level for comparison. However, the International Water Management Institute (IWMI) recently completed a Global Irrigated Area Map (GIAM) using 10x10-$km^2$ Advanced Very High Resolution Radiometer (AVHRR), SPOT vegetation monthly NDVI, 1x1-$km^2$ GTOPO30 Digital Elevation Model, 1x1-$km^2$ AVHRR forest cover, and historical monthly precipitation data. We evaluated the MIrAD-US map based on a comparison with GIAM. These two maps have some key differences: they represent irrigated areas for two different years (2002 for MIrAD-US and 1999 for GIAM), they have different spatial resolutions and classification schemes, and they are based on different methodologies. Due to these differences in the maps' characteristics, we compared county-summarized irrigated-area information (expressed as a fraction) extracted from these two maps based on their spatial autocorrelation in contrast with traditional assessment methods. We used a regionalized approach to analyze regional variations in spatial autocorrelation in the maps. In the western states, the maps were more similar where irrigation is found in large, relatively homogeneous spatial clusters, but the maps differed across the central and Mississippi Flood Plain (MFP) states where irrigation is more scattered and sparse with relatively smaller farm sizes. For total irrigated areas, GIAM represented 22.3% lower, 64.5% higher, and 54.2% higher in the western, central, and MFP regions, respectively, compared to USDA statistics. We concluded that the resolution of the source satellite data for GIAM may be one reason for these large differences in irrigated areas. While evaluating the consistency of mapped irrigated areas by these two maps, both maps were found to be consistent; however, MIrAD-US exhibited better agreement with historical rainfall patterns for the western and central regions.

## INTRODUCTION

The characterization of irrigated areas across large geographic areas presents many unique challenges for the validation and comparison of map products. It is often difficult to obtain a similar map from a second source that shares similar spatial and temporal characteristics. Inconsistency in derived map products is expected when the various components of map production are considered: data inputs, preprocessing techniques, classification methods, ancillary data, and thematic legends, which all eventually lead to differences in the final thematic map (Wulder et al., 2004). In addition, rigorous accuracy assessment based on ground truth is constrained by the lack of comprehensive ground data, logistical realities, and high monetary costs (Merchant et al., 1994; Muchoney et al., 1999). Notably, map characteristics are the direct product of specific project objectives. For instance, both the MODIS Irrigated Agriculture Dataset for the United States (MIrAD-US) and the Global Irrigated Area Map (GIAM; Thenkabail et al., 2006) mapped irrigated areas, but the prime objective for MIrAD-US was to map irrigated areas as a single class only in the United States, whereas the objective of GIAM was to map different types of irrigated lands around the world. Thus, differing project objectives will invoke differing outcomes.

Recently, we produced MIrAD-US dataset at U.S. Geological Survey Earth Resources Observation and Science Center using time-series 250x250-$m^2$ Moderate Resolution Imaging Spectroradiometer (MODIS; Justice and Townshend, 2002) satellite-derived vegetation index [Normalized Difference Vegetation Index (NDVI)] observations, U.S. Department of Agriculture (USDA) county-level irrigation summary statistics for 2002 (USDA-NASS, 2004), and 2001 National Land Cover Database (2001 NLCD; Homer et al., 2004). We developed an automated classification routine where the cells with the highest peak NDVI within the land cover masked cells in a county that were identified as irrigated lands, and the accumulated area covered by those pixels was calculated. Then, this accumulated area was compared with the target number of acres provided by the 2002 Census of Agriculture. If the total area of the selected cells was under the target area, then cells with the next highest annual peak NDVI were selected, and the accumulated area of the cells identified by the two highest annual peak NDVI values were then compared with the target number of irrigated acres for the county. These steps were repeated until the target area for the county was exceeded. In a final step, all lone 250x250-$m^2$ pixels were filtered from the irrigated cells based on the assumption that, in the United States, irrigated fields are generally larger than 62,500 $m^2$ (15.4 acres/6.3 ha). The process was run iteratively county by county. The resulting irrigated area map is referred to as MIrAD-US (Figure 1). Another irrigated map known as GIAM was produced by International Water Management Institute (IWMI). GIAM was the first attempt to map global irrigation incorporating satellite observations for the year 1999. It incorporated eight classes of irrigated areas through an unsupervised classification routine involving 10x10-$km^2$ Advanced Very High Resolution Radiometer (AVHRR), SPOT vegetation monthly NDVI, 1x1-$km^2$ GTOPO30 Digital Elevation Model, 1x1-$km^2$ AVHRR forest cover, and historical monthly precipitation data. The final map was downscaled to a 1x1-$km^2$ resolution with fractional irrigation expressed in each cell for each of these eight classes. The primary purpose of this paper is to compare the area and spatial agreement of the irrigated areas identified in these two maps.

## METHODS

Despite the differences in temporal, spatial, and thematic characteristics, we choose GIAM to perform a comparison with MIrAD-US, because no other comparable maps of irrigated areas at national scale exist for the United States. Both maps may be considered correct and accurate by the map's objective measurements. The comparison is not to identify which map is the most accurate; rather it is to assess the similarities and differences in spatial distribution and to identify potential regional strengths and weaknesses. Therefore, we performed spatial autocorrelation, linear regression, and simultaneous autoregression methods instead of traditional methods of map comparison for addressing and quantifying the locations and magnitude of the similarities and differences, because the traditional cell-by-cell analysis would be challenging to interpret similarities and differences considering the inherent differences in characteristics of these two datasets. We applied Moran's statistics to analyze the spatial distribution patterns and spatial structures of the irrigated areas across the region from both maps, the linear regression quantified the relationship in magnitude of the irrigated areas from these two maps, and the autoregresson quantified the relationship of the spatial distribution of irrigated areas from these two maps with historical average rainfall pattern.

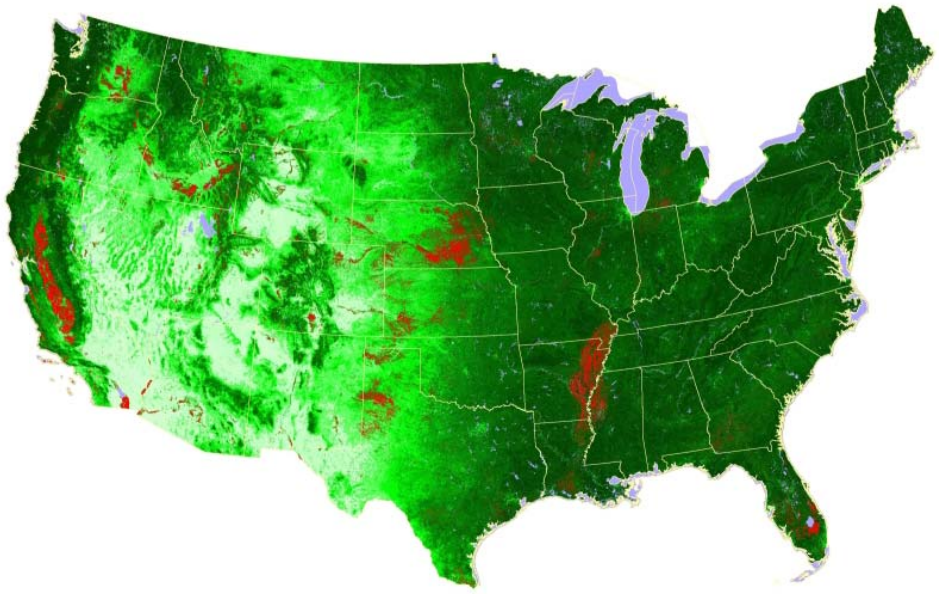

**Figure 1.** The MIrAD-US map. Irrigated pixels are shown in red on a background showing peak vegetation growth (i.e., annual maximum NDVI).

## Study Area

In consideration of regional differences in irrigation practices across the United States, we used a regional framework for comparison. Four regions (Figure 2) were identified (western, central, Mississippi Flood Plain (MFP), and eastern) based on the primary water source for irrigation, climate, geographic homogeneity, and extent of the groundwater aquifer (where groundwater was the main source). Surface water is the primary source for irrigation in the intermountain west, whereas groundwater is the main source for irrigation in the central region (Hutson et al., 2004). The eastern United States is comparatively humid, and irrigation is less prevalent in this part of the country except for some areas in the MFP and in Florida. Groundwater is also the main source of irrigation for the MFP region (Hutson et al., 2004). Three of these regions (western, central, and MFP) include 18 of the 20 states with the largest numbers of irrigated acres according to the 2002 Census of Agriculture (Veneman et al., 2002). The eastern region was not yet considered in this analysis but will be analyzed at a future date.

## Data Preparation

Data preparation steps included reprojection and appropriate fraction coefficient computation for the GIAM data layer, calculation of the fraction of irrigated area by county, or County Irrigated Area Fraction (CIAF), and data normalization. The GIAM data layer was reprojected to Lambert Azimuthal Equal Area projection to match the coordinate system of the MIrAD-US data set. In the United States, most irrigation is generally delivered in a single season (Hutson et al., 2004), so the fraction coefficient (Thenkabail et al., 2006) derived by combining Google Earth, high-resolution imagery, and fallow was applied. GIAM's eight irrigation classes were merged into a single irrigation category. Using U.S. counties (administrative units) as the spatial unit for this comparison, the CIAF, the fractional area of each county designated as irrigated, was derived from both maps. An *arcsin square root* transformation was applied to the CIAF summaries from GIAM and MIrAD-US to ensure that the data were normally distributed (Anselin, 1992) and to provide a remedy for outliers and skewness in each distribution.

An ArcInfo shapefile format was used to manage the CIAF computed from GIAM and MIrAD-US for the three regions of analysis. We used the R statistical software package to investigate the spatial autocorrelation of each regional irrigation data set and to compare the MIrAD-US and GIAM.


**Figure 2.** Analysis regions based on main irrigation water source, climate, geographic heterogeneity, and extent of the groundwater aquifer.

## RESULTS AND DISCUSSIONS

### Distribution Patterns of Irrigated Areas in MirAD-US and GIAM

We used Moran's scatterplots to analyze the distribution patterns of the irrigated areas as summarized by county (i.e., CIAFs) from both maps. Moran's scatterplot describes an observation with respect to its surrounding neighbor's observations. It is a plot of $x_i$ (the value at each county) versus $\sum w_{ij} x_j$, which is the weighted average of the $x_i$ value based on neighbors (O'Sullivan and Unwin, 2002). The scatterplots for all three regions show evidence of spatial autocorrelation for CIAF in both maps, indicating that irrigated areas were mainly mapped in clustered patterns. Figures 3a and 3b present very similar spatial distribution characteristics for irrigated areas in the western region. For both maps, the numbers of counties with low CIAF surrounded by the low weighted average of CIAF for neighboring counties (in other words, the low-low distribution) were high, and there were relatively few counties with high CIAF surrounded by the high weighted average of CIAF for neighboring counties (that is, high-high distribution). This suggests that both maps effectively mapped irrigation patterns with similar types of spatial distributions. In the western region, average farm sizes were larger and over 50% of the farms were irrigated (Table 1), so irrigation occurred at relatively larger scales/clusters in this region according to the USDA Census of Agriculture. This appears to support the distribution pattern result (Figures 3a and 3b). In other words, the spatial autocorrelation characteristics, or pattern of distribution, of both data sets are similar.

**Table 1.** Farm size and number of irrigated farms from the 2002 Census of Agriculture (USDA-NASS, 2004).

| Region | Average farm size (acres/ha) | Farms with irrigation (%) | Total no. of farms | No. of irrigated farms |
|---|---|---|---|---|
| Western | 813.5/329.2 | 50.4 | 264,674 | 133,356 |
| Central | 799.6/323.6 | 15.0 | 513,692 | 76,842 |
| MFP | 264.4/107 | 4.0 | 779,963 | 31,189 |

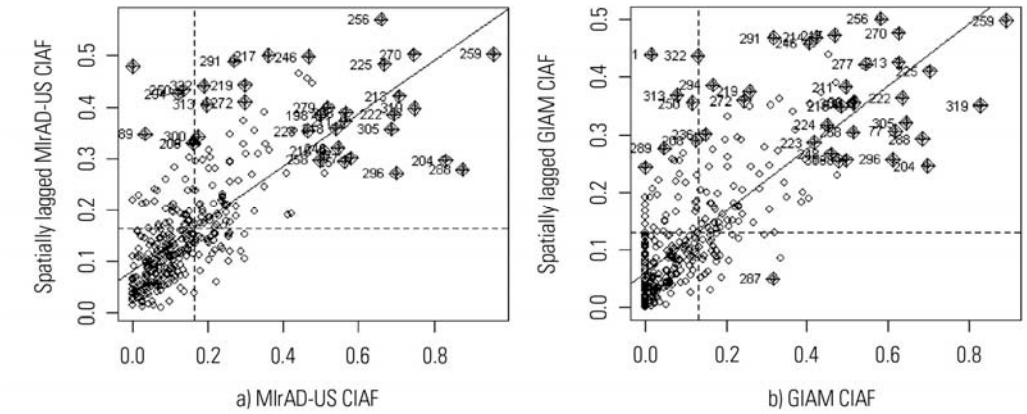


**Figure 3.** Distribution pattern of irrigated areas by county in the western region, a) CIAF extracted from MIrAD-US, b) CIAF extracted from GIAM

The central region shows markedly different distribution patterns from the western region in the two maps. Figures 4a and 4b show that the low-low distribution was high for MIrAD-US but comparatively low for GIAM. On the other hand, the high-high distribution was comparatively low for MIrAD-US but high for GIAM. This difference in the two CIAF distributions indicates that the MIrAD-US was effective at mapping sparsely irrigated areas across the central region, whereas GIAM appeared to be less successful at mapping sparse irrigation and predominantly captured larger, spatially aggregated irrigated areas in the region.

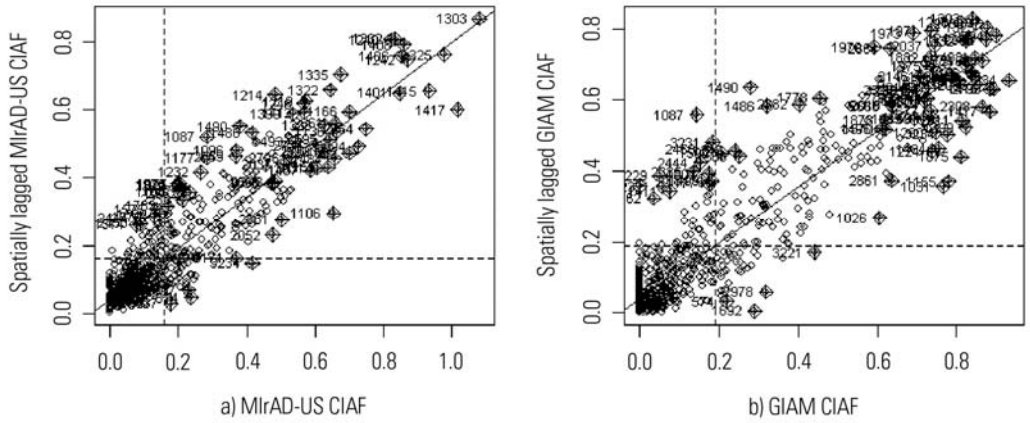


**Figure 4.** Distribution pattern of irrigated areas by county in the central region, a) CIAF extracted from MIrAD-US, b) CIAF extracted from GIAM**.**

In the MFP region, the low-low distribution was again comparatively high, while the high-high distribution was low (Figures 5a and 5b) for the MIrAD-US. The high-high distribution was high for GIAM, which indicated that the total number of counties with high CIAF was higher in the GIAM data set than that of the MIrAD-US data.

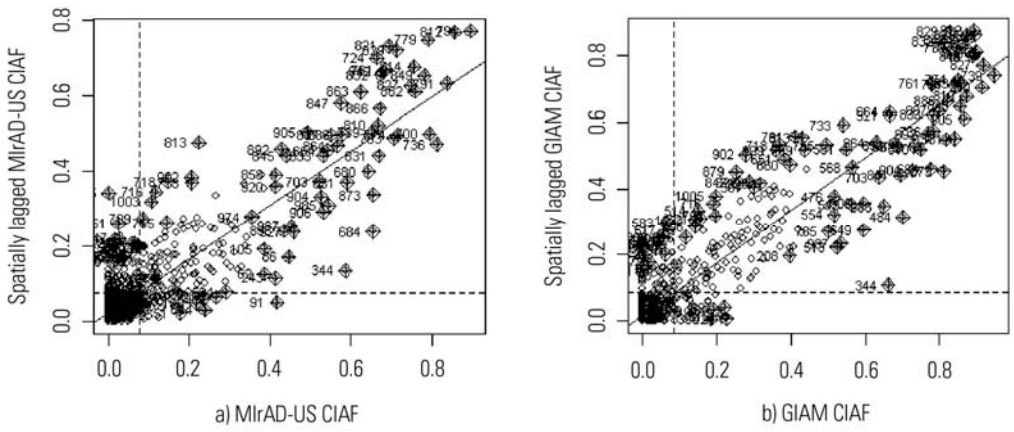


**Figure 5.** Distribution pattern of irrigated areas by county in the MFP region, a) CIAF extracted from MIrAD-US, b) CIAF extracted from GIAM.

## MIrAD-US and GIAM Spatial Structure

Moran's I correlograms provided information on the spatial patterns of irrigation in the CIAF distributions for both maps. The correlogram provides an indication of the extent of significant spatial clustering of similar values around any set of observations (Barbaro et al., 2007). The correlograms for the western region for CIAF in Figures 6a and 6b showed very similar structures of spatial clustering up to the third order of neighbors from both maps. The similar Moran's I values in the correlograms between lag 4 and 7 indicate significant autocorrelation of similar values in a linear pattern, which corresponds well with the high density of irrigation in the central valley counties of California, which are oriented in a north-south linear pattern.

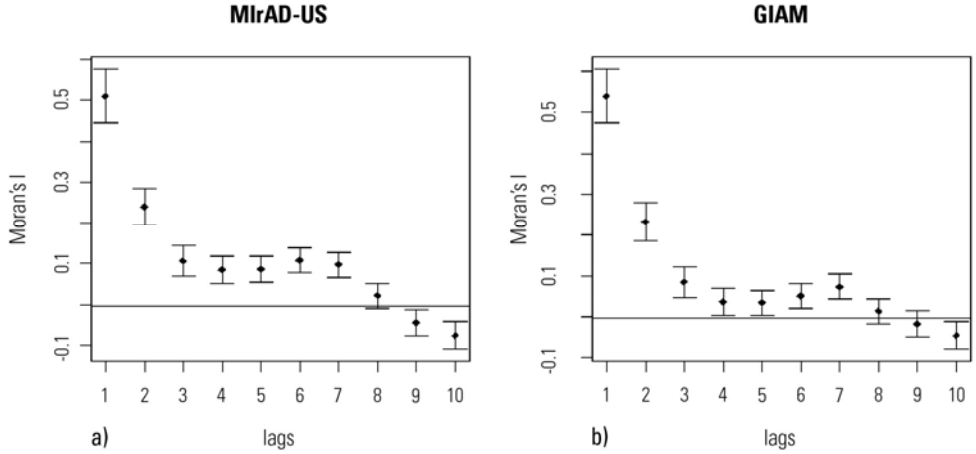


**Figure 6.** Moran's I correlograms showing pattern of spatial clustering in the western region a) from MIrAD-US, b) from GIAM.

In Figures 7a and 7b, the correlograms for the central region indicate the extent of spatial clustering for the CIAF as it increases to the sixth-order neighbors in the MIrAD-US and to the fifth-order neighbors in the GIAM. These indicate that for the central region, cluster sizes are comparatively bigger for MIrAD-US CIAF than for GIAM CIAF. However, for MFP region, Figures 8a and 8b indicate the opposite.

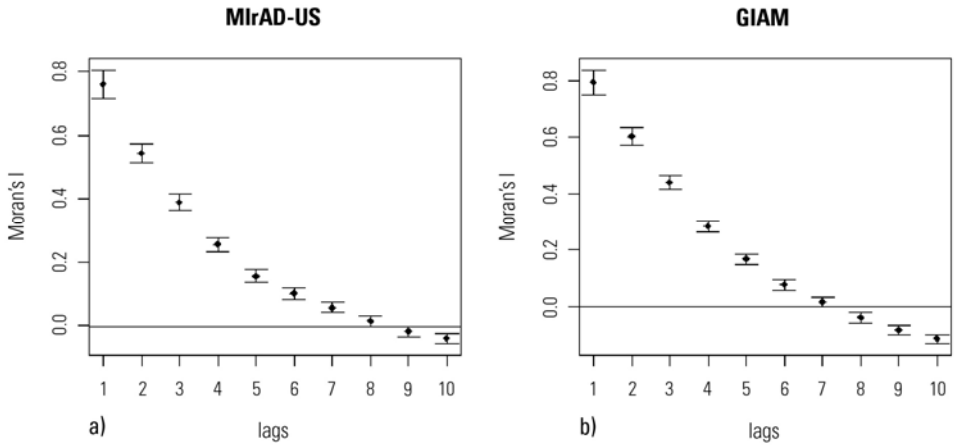


**Figure 7.** Moran's I correlograms showing pattern of spatial clustering in the central region, from a) MIrAD-US, and b) GIAM.

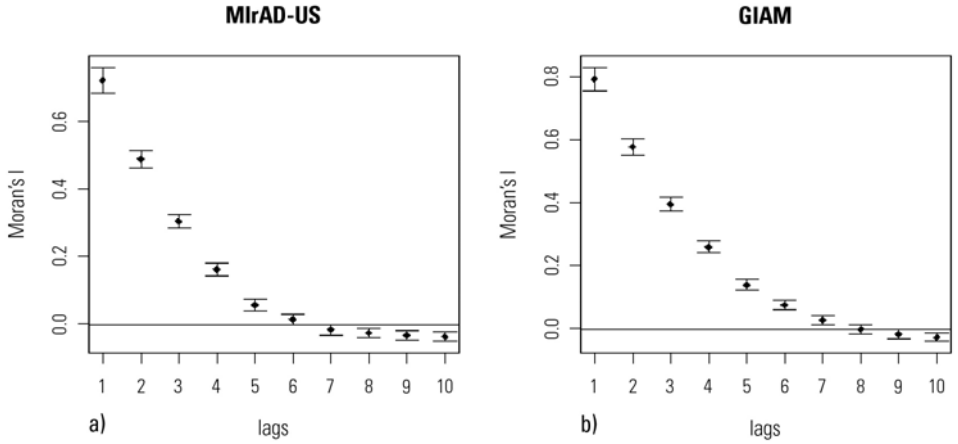


**Figure 8.** Moran's I correlograms showing pattern of spatial clustering in the MFP region, from a) MIrAD-US, and b) GIAM.

## Area Comparison to USDA-NASS Irrigation Statistics

Table 2 presents the statistics of the irrigated area in each county from MIrAD-US, GIAM, and 2002 USDA Census of Agriculture (USDA-NASS, 2004) summarized by region. The MIrAD-US was derived using the county irrigated area statistics of 2002 USDA Census of Agriculture, so these two data sets are not independent of each other. But statistics computed from independently derived GIAM are comparable to USDA statistics. In the western region, the irrigated area identified by USDA was 83,600 km$^2$ (about 3.47% of the total area in the region). In comparison, the GIAM irrigated area was 64,900 km$^2$ (about 2.7% of the total area in the region). For the western region, the GIAM irrigated area was 22.5% less than that given by the 2002 USDA Census of Agriculture (USDA-NASS, 2004) and MIrAD-US. The central region GIAM irrigated area estimate was 141,400 km$^2$, or 64.5% higher than the USDA areal estimate (86,000 km$^2$) and 62% higher than the MIrAD-US estimate (87,300 km$^2$). GIAM estimated 6.1% of the entire region as irrigated, while MIrAD-US and the USDA estimated 3.7% of the area as irrigated. The MIrAD-US and USDA statistics reported 39,600 km$^2$ and 36,600 km$^2$ of irrigated area in the MFP region, but the GIAM estimate was 56,400 km$^2$, or 42% and 54% higher than the MIrAD-US and USDA areal estimate. Based on these statistics, the most significant differences in irrigated area statistics are in the central and MFP region where GIAM estimates were higher than the estimates from MIrAD-US and USDA statistics. Using the local Moran's I statistic (O'Sullivan and Unwin, 2002; Overmars et al., 2003) and regression model (O'Sullivan and Unwin, 2002) we further analyzed the spatial distribution and magnitude of these differences focusing on the GIAM and MIrAD-US.

**Table 2.** Comparison of irrigated area statistics of MIrAD-US, GIAM, and USDA 2002 Census of Agriculture.

| | Western region | | | Central region | | | MFP region | | |
|---|---|---|---|---|---|---|---|---|---|
| | MIrAD-US | GIAM | USDA | MIrAD-US | GIAM | USDA | MIrAD-US | GIAM | USDA |
| Irrigated area (area in $km^2$) | 83,849 | 64,972 | 83,625 | 87,319 | 141,469 | 86,013 | 39,679 | 56,466 | 36,609 |
| % of the total area | 3.5 | 2.7 | 3.4 | 3.7 | 6.1 | 3.7 | 2.6 | 3.7 | 2.4 |
| % difference from USDA statistics | 0.3 | -22.3 | - | 1.1 | 64.5 | - | 8.5 | 54.2 | - |

## Areas of Agreement and Disagreement

The local Moran's I (Equation 1) statistic map of Local Indicator of Spatial Association (LISA) provided an indication of locations of hot spots, or spatial high-density clusters of similar values.

Equation 1: Local Moran's I

$$I_{local} = (x_i - \bar{x})\sum_{j=1}^{n} w_{ij}(x_j - \bar{x})$$

where $x_i$ is the observation (CIAF), $\bar{x}$ is the mean of the observations, $w_{ij}$ is the weight, and $x_j$ is the neighbor's observation. The values of Moran's I generally vary between 1 and -1. Positive autocorrelation in the data translates into positive values of *I*; negative autocorrelation produces negative values. Values close to zero indicate no autocorrelation (Overmars et al., 2003). The maps of local Moran's I for GIAM and MIrAD-US can be subsequently compared visually for the geographic patterns of similarity and dissimilarity. The western region maps of local Moran's I (Figures 9a and 9b) show generally strong agreement in the higher density irrigated counties in California, Washington, and Idaho. In the central region, the agreement is good in parts of the irrigated counties in Nebraska and Texas, but it is poor for western Kansas (Figures 9c and 9d) where the GIAM data set indicates a much higher density of irrigated lands. The central region maps also show evidence of magnitude differences in irrigated areas within the clusters of high-density irrigation in Nebraska.

In the MFP region (Figures 9e and 9f), the LISA maps show close agreement for the cluster of irrigated acres covering parts of Missouri, Arkansas, Mississippi, and Louisiana. However, GIAM identified a few clusters of irrigated acres in southern Illinois and central Iowa where MIrAD-US did not, and the MIrAD-US irrigated area map identified a cluster of irrigation in northern Indiana. The LISA maps provided an effective and heuristic tool for qualitative comparison and visual assessment of spatial clustering of irrigated areas from both the GIAM and the MIrAD-US, but the maps do not support a quantitative evaluation of spatial agreement.

## Quantifying the Agreement Between MIrAD-US and GIAM

To quantify the spatial agreement in irrigated areas from both maps, an Ordinary Least Square (OLS) regression model was applied (Equation 2).

Equation 2. The OLS regression

$$y = \beta_0 + x\beta_1 + \varepsilon$$

where $y$ is the dependent variable, $x$ is the independent variable, $\beta_0$ is the constant, $\beta_1$ is the model coefficient, and $\varepsilon$ is the noise. The OLS regression model was fit taking the GIAM CIAF as the dependent variable and MIrAD-US CIAF as the independent variable. The model coefficients and associated p-values for all the regions are presented in Table 3. The p-value determines the statistical significance of the coefficients ($\infty <= 0.05$), and the coefficient of determination ($r^2$) provides the portion of total variation explained by the regression equation. The western region shows the highest $r^2$ of 0.80, which suggests a fairly strong agreement between MIrAD-US CIAF and GIAM CIAF. But the agreements were weaker for the central ($r^2 = 0.63$) and MFP regions ($r^2 = 0.58$).

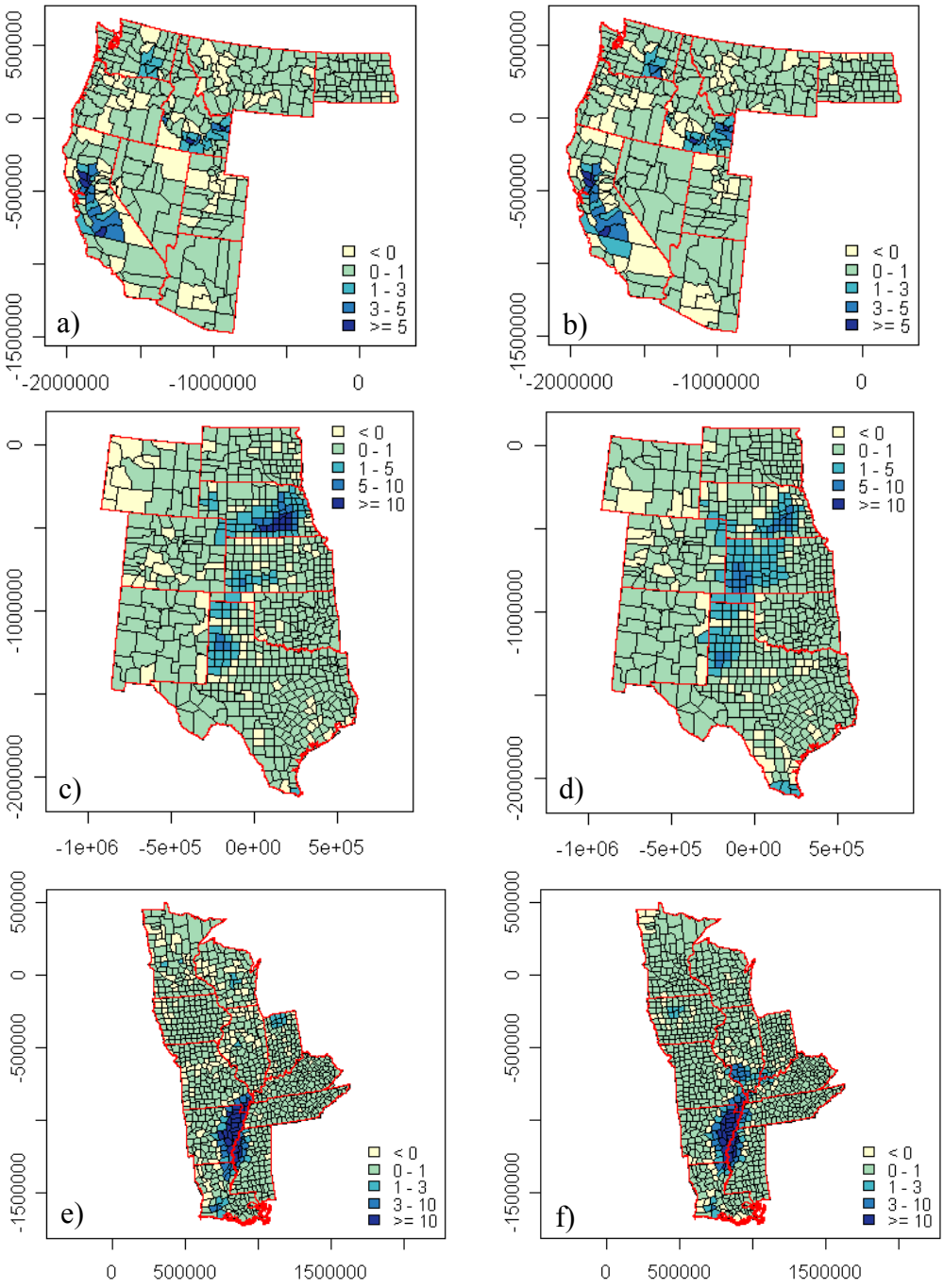


**Figure 9.** The local Moran's statistic maps of LISA for the western region (a) MIrAD-US CIAF, (b) GIAM CIAF; the central region, (c) MIrAD-US CIAF, (d) GIAM CIAF; and the MFP region (e) MIrAD-US CIAF, and (f) GIAM CIAF.

**Table 3.** The OLS model coefficients and associated p-values.

| Parameters | Western region | | Central region | | MFP region | |
|---|---|---|---|---|---|---|
| | Value | P-value | Value | P-value | Value | P-value |
| Slope ($\beta_1$) | 0.90 | ~0 | 1.09 | ~0 | 1.00 | ~0 |
| $R^2$ | 0.80 | | 0.63 | | 0.58 | |

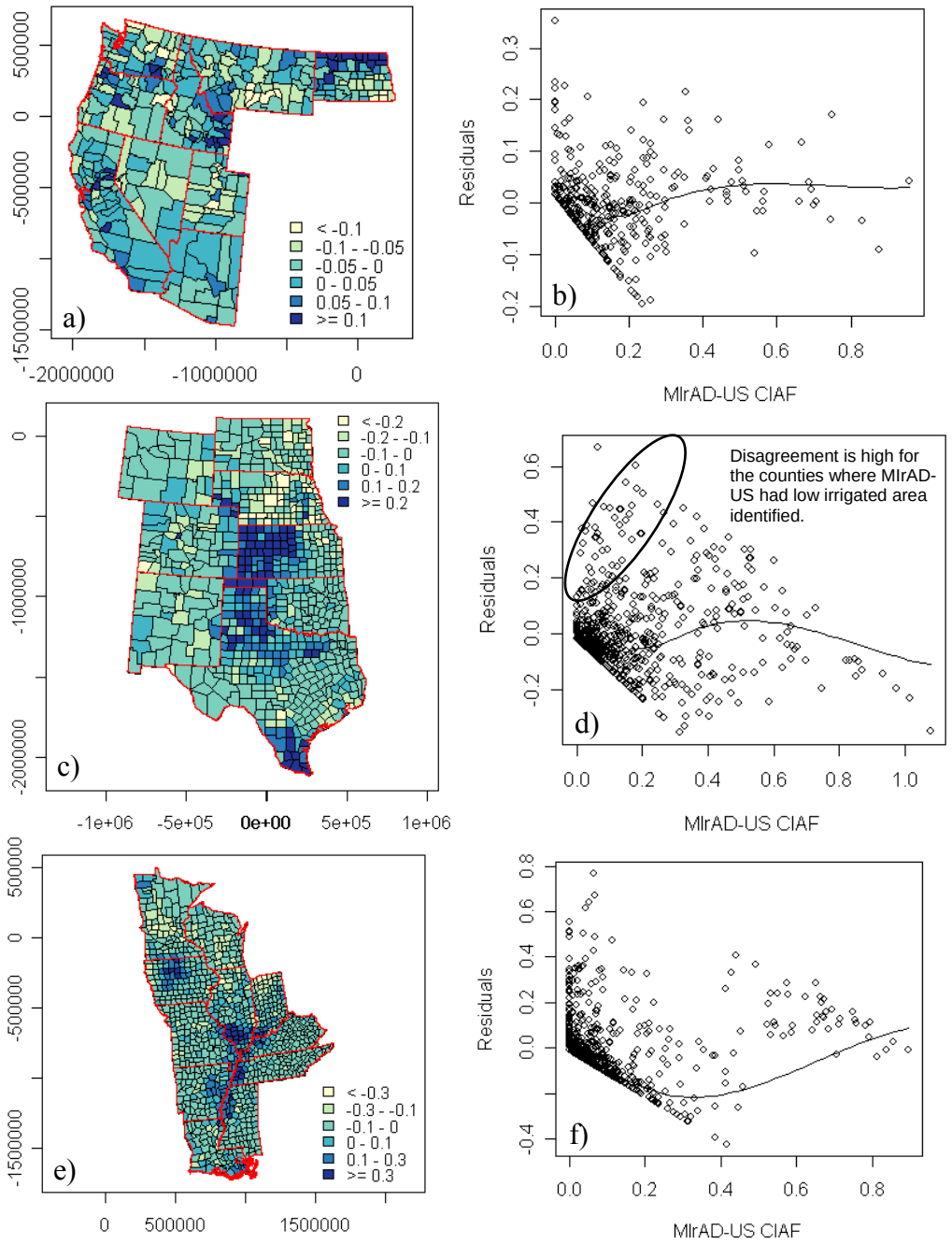


**Figure 10.** (a) The OLS regression residuals map, and (b) scatterplot of MIrAD-US CIAF and OLS residuals for the western region; (c) the OLS regression residuals map, and (d) scatterplot of MODIS CIAF and OLS residuals for the central region; and (e) the OLS regression residuals map, and (f) scatterplot of MODIS CIAF and OLS residuals for the MFP region.

For each region, areas of spatial agreement and disagreement were analyzed with the help of the OLS residuals maps and scatterplot of residuals versus independent variable (MIrAD-US) (in other words, counties where GIAM overestimated or underestimated irrigated areas compared to the irrigated areas from MIrAD-US). In the residuals maps (Figures 10a, 10c, and 10e), counties with positive values identify areas where GIAM overestimated irrigated acres compared to MIrAD-US, and counties with lower negative values show where GIAM underestimated irrigated acres. The residuals map and scatterplot in Figures 10a and 10b show comparatively low residuals occurring randomly across the western region without any trend except for North Dakota. The GIAM map produced CIAF

estimates in northern counties of North Dakota were 10% or greater compared to the CIAF estimates from MIrAD-US in those counties.

In the central region, the autocorrelated residuals were high for some counties in Nebraska, Kansas, and Texas. Figure 10c shows that, compared to MIrAD-US, irrigated areas from GIAM were higher by 20% or more for some counties in Kansas and Texas, but it was lower by 20% or more for a few counties in Nebraska. It was observed that GIAM and MIrAD-US have higher agreement for counties where the fraction of irrigated acres was high in both data sets. But where the county irrigated area estimates were small in MIrAD-US, GIAM had the tendency to either estimate a much higher irrigated fraction or to estimate none (zero) (Figure 10d). These results indicate that the MIrAD-US model had a better capability of mapping geographically sparse irrigation, whereas the GIAM strategy mapped the larger clusters of irrigated areas fairly well in the central region. This is likely due to the finer resolution and improved detail of the 250x250-$m^2$ MODIS data input into the MIrAD-US model.

In the MFP region (Figure 10e), GIAM overestimated irrigated areas by 30% or more for some counties in Iowa, Illinois, and Tennessee, and for a few random counties in Minnesota and Indiana, it underestimated irrigated areas by 30% or more.

## Consistency in Spatial Distribution

In an effort to evaluate the consistency of spatial distribution of MIrAD-US and GIAM, we compared the spatial distribution of irrigated areas extracted from these two maps with spatial distribution of historical annual precipitation. Our assumption was that the irrigated areas would be geographically located in areas with low precipitation. This assumption is supported by the facts for the United States where irrigated lands are predominantly located in the areas where average annual precipitation is typically less than 508 mm and is insufficient to support crops without supplemental water (Hutson et al., 2004). We used 30-year (1971-2000) annual average precipitation (Daly et al., 2002) data downloaded from the Parameter-elevation Regressions on Independent Slopes Model (PRISM) group web portal at Oregon State University (http://www.prismclimate.org) to evaluate the spatial distribution patterns. A *log* transformation was applied to the precipitation data to ensure that the data were normally distributed and as a remedy for outliers and skewness in the distribution (Anselin, 1992). We applied a simultaneous autoregressive (SAR) model (Anselin, 2002; Overmars et al., 2003) to evaluate the spatial distribution patterns. We expected a negative relationship between irrigated areas and precipitation; for example, higher density in irrigated lands would be located in geographical areas with lower average annual precipitation and vice versa. Equation 2. Simultaneous Autoregressive (SAR) regression

$$(1-\rho W)y = (1-\rho W)X\beta + \varepsilon$$

where $\rho$ is the autoregressive parameter, $W$ is the spatial weight matrix, $y$ is the dependent variable, $X$ is the independent variable, $\beta$ is the coefficient, and $\varepsilon$ is the noise. This is basically a regression performed on a spatially filtered independent variable (Anselin, 2002). Table 4 presents the SAR model coefficients for all three regions. The lower Akaike Information Criterion (AIC) values suggest an improved fit for SAR compared to the linear model (Anselin, 2002). The model coefficients ($\beta$) show that average annual precipitation was indeed negatively correlated with irrigated areas in both maps for western and central region. The model coefficients were not statistically significant (p-value < 0.05) for the MFP region. Based on the model coefficient values, we concluded that the MIrAD-US map is more consistent with the precipitation pattern in the western and central regions compared to that of GIAM. As the MFP region is more humid and experiences relatively higher precipitation compared to western and central regions, both the MIrAD-US and GIAM do not correlate well with the precipitation pattern.

**Table 4.** Simultaneous Autoregressive (SAR) model coefficients and associated values for CIAF as a function of historical annual average precipitation.

| Regions | Source map | $\beta$ | P-value | $\rho$ | AIC | Linear model |
|---|---|---|---|---|---|---|
| Western | MIrAD-US | -0.156 | 2.39E-13 | 0.850 | -506.1 | -291.7 |
| | GIAM | -0.132 | 3.93E-10 | 0.839 | -508.8 | -278.7 |
| Central | MIrAD-US | -0.128 | 0.0002 | 0.924 | -1436.2 | -541.4 |
| | GIAM | -0.087 | 0.060 | 0.925 | -1058.4 | -155.8 |
| MFP | MIrAD-US | -0.002 | 0.344 | 0.907 | -2292.2 | -1206.1 |
| | GIAM | na | na | na | -2132.1 | -564.3 |

## CONCLUSIONS

Comparison of remote sensing-based maps with differences in spatial and temporal characteristics and creation methods is a challenge. In this comparison, as opposed to conventional assessment methods, we used geospatial analysis techniques of spatial autocorrelation to compare irrigated information derived from two national-level maps of irrigated areas from two different sources. Using a regional approach, the MIrAD-US and GIAM maps agreed the best in the western region where irrigation patterns are relatively homogeneous across comparatively large farms. But the maps differed for the central and MFP regions where irrigation is more scattered and sparse and the average farm sizes are smaller. For these two regions, GIAM mapped more irrigated areas compared to MIrAD-US. The agreement was good for much of the western region with the exception of the northern border of North Dakota and eastern edge of Idaho. In the central region, the maps agreed well for much of Wyoming, Colorado, New Mexico, Oklahoma, and eastern Kansas, but they did not agree well for western Kansas, southern and panhandle Texas, and central Nebraska. In the MFP region, the maps agreed well for the northern, eastern, and southwestern edges of the region but did not agree well for southern Illinois and parts of Iowa. The GIAM-mapped irrigated area was 22.3% lower in the western region, 64.5% higher in the central region, and 54.2% higher in the MFP region compared to the irrigated areas reported by USDA Census of Agriculture for those regions. We concluded that the coarse spatial resolution (10x10 $km^2$) of the source data for GIAM may be the reason for these large differences in irrigated areas. To evaluate the consistency of the spatial distribution of irrigated areas in those two maps, we compared the spatial distribution of MIrAD-US and GIAM with the spatial distribution of historical precipitation assuming that the irrigated areas would be geographically located in the areas with lower precipitation that require supplemental water to support crops. Both maps were consistent with precipitation patterns, with MIrAD-US exhibiting a stronger relationship than GIAM over all three regions, and the relationship was the strongest in the climatically arid western region.

The techniques of spatial autocorrelation used in the analysis to evaluate the maps were very helpful. The Moran's scatterplots explained the distribution pattern of associated irrigated information, and local Moran's I statistic maps identified the geographic locations of spatial agreement and disagreement. The OLS regression model quantified the correlation in geospatial information, whereas the autoregression model identified the strength of the relationship between geospatial variables. These geospatial analysis techniques provided effective heuristic tools for comparing geospatial information derived from raster maps with differences in spatial resolutions and classification methods.

## LIMITATIONS AND FUTURE DIRECTIONS

Counties were the spatial units for this comparison and they vary substantially in size across the United States. Counties are relatively smaller in the east than in the west. Thus, the associated data sets of these counties were subject to a Modifiable Area Unit Problem (MAUP). We did not investigate the effects of MAUP on the spatial autocorrelation. Geospatial tools (e.g. Moran's I ) assume that data is distributed normally, thus there were violations of this assumption. In addition, we did not account for the temporal mismatch between GIAM and MIrAD-US in this analysis. We assumed that this effect was insignificant because recent trends in irrigated acres appear to be holding steady for the United States (Veneman et al., 2004).

We plan to perform a traditional method of map comparison (e.g., dot grid approach) to evaluate MIrAD-US and GIAM. Plans are also underway to perform state level evaluation of MIrAD-US using best available state level irrigation maps with similar or greater mapping details, primarily focusing on the states with the largest number of irrigated acres.

## ACKNOWLEDGMENTS

The MODIS time-series data set used in this research was created at the Kansas Applied Remote Sensing Program at the University of Kansas through funding from the USGS AmericaView Program (Grant # AV04-KS01) and the Department of the Army (Grant # 911SR-04-C-0006). The authors thank Ronald Smith, USGS, for the calculation of the land cover mask. Any use of trade, product, or firm names is for descriptive purposes only and does not imply endorsement by the U.S. Government.

## REFERENCES

Anselin, L., 1992. *Spacestat Tutorial. A Workbook for Using Spacestat in the Analysis of Spatial Data.* University of Illinois, Urban-Champaign, pp. 167.

Anselin, L., 2002. Under the hood issues in the specification and interpretation of spatial regression models. *Agricultural Economics, 27*(3):247-267.

Barbaro, L., J.P. Rossi, F. Vetillard, J. Nezan, and H. Jactel, 2007. The spatial distribution of birds and carabid beetles in pine plantation forests: the role of landscape composition and structure. *Journal of Biogeography, 34*(4):652–664.

Daly, C., W.P. Gibson, G.H. Taylor, G.L. Johnson, and P. Pasteris, 2002. A knowledge-based approach to the statistical mapping of climate. *Climate Research, 22*:99-113.

Homer, C., C. Huang, L. Yang, B. Wylie, and M. Coan, 2004. Development of a 2001 National Landcover Database for the United States. *Photogrammetric Engineering and Remote Sensing, 70*(7):829-840.

Hutson, S.S., N.L. Barber, J.F. Kenny, K.S. Linsey, D.S. Lumia, and M.A. Maupin, 2004. Estimated use of water in the United States in 2000, Reston, Virginia., U.S. Geological Survey Circular 1268.

Justice, C.O., and J.R.G. Townshend, 2002. Special issue on the Moderate Resolution Imaging Spectroradiometer (MODIS): A new generation of land surface monitoring. *Remote Sensing of Environment*, *83*:1-2.

Merchant, J.W., L. Yang, and W. Yang, 1994. Validation of continental-scale land cover data bases developed from AVHRR data. *In Proceedings of the Pecora 12 Symposium, Land Information from Space Based Systems,* 24-26 Aug. 1993, Sioux Falls, SD. American Society for Photogrammetry and Remote Sensing (ASPRS), Bethesda, MD, 201-205.

Muchoney, D., A. Strahler, J. Hodges, and J. LoCastro, 1999. The IGBP DiSCover confidence sites and the system for terrestrial ecosystem parameterzaion: tools for validation global land-cover data. *Photogrammetric Engineering and Remote Sensing, 65*(9):1061-1067.

O'Sullivan, D., and Unwin, D.J., 2002. *Geographic Information Analysis,* John Wiley & Sons, Inc., Hoboken, NJ.

Overmars, K.P., G.H.J. de Koning, and A. Veldkamp, 2003. Spatial autocorrelation in multi-scale land use models. *Ecological Modelling, 164*(2-3):257-270.

Thenkabail, P.S., C.M. Biradar, H. Turral, P. Noojipady, Y.J. Li, J. Vithanage, V. Dheeravath, M. Velpuri, M. Schull, X.L. Cai, and R. Dutta, 2006. An Irrigated Area Map of the World (1999) derived from Remote Sensing, Research Report # 105, International Water Management Institute, Colombo, Sri Lanka [http://www.iwmigiam.org].

USDA-NASS, 2004. U.S. Department of Agriculture, National Agricultural Statistics Service, 2002 Census of Agriculture, Summary and state data, Volume 1, Geographic Area Series, Part 51, AC-02-A-51. [http://www.nass.usda.gov/census/census02/volume1/us/USVolume104.pdf].

Veneman, A.M., J.J. Jen, and R.R. Bosecker, 2004. 2002 Census of Agriculture—Farm and Ranch Irrigation Survey (2003), Volume 3, Special Studies, Part 1, U.S. Department of Agriculture, National Agricultural Statistics Survey (NASS). [http://www.agcensus.usda.gov/Publications/2002/FRIS/fris03pdf].

Wulder, M.A., D. Seemann, and J.C. White, 2004. Map comparison using spatial autocorrelation: an example using AVHRR derived land cover of Canada. *Canadian Journal of Remote Sensing, 30*(4):573-592.